CHIN. PHYS. LETT. Vol. 37, No. 6 (2020) 060301

Dynamics of the Entanglement Spectrum of the Haldane Model under a Sudden Quench *

Lin-Han Mo(莫林翰)[1], Qiu-Lan Zhang(张秋兰)[2**], Xin Wan(万歆)[1,3]

[1]*Zhejiang Institute of Modern Physics, Zhejiang University, Hangzhou 310027, China*
[2]*School of Information Science and Engineering, Zhejiang University Ningbo Institute of Technology, Ningbo 315100, China*
[3]*CAS Center for Excellence in Topological Quantum Computation, University of Chinese Academy of Sciences, Beijing 100190, China*

(Received 26 March 2020)

One of the appealing features of topological systems is the presence of robust edge modes. Under a sudden quantum quench, the edge modes survive for a characteristic time that scales with the system size, during which the nontrivial topology continues to manifest in entanglement properties, even though the post-quench Hamiltonian belongs to a trivial phase. We exemplify this in the quench dynamics of a two-dimensional Haldane model with the help of one-particle entanglement spectrum and the probability density of its mid-states. We find that, beyond our knowledge in one-dimensional models, the momentum dependence of the transverse velocity plays a crucial role in the out-of-equilibrium evolution of the entanglement properties.

PACS: 03.65.Vf, 03.65.Ud DOI: 10.1088/0256-307X/37/6/060301

Since the discovery of the integer quantum Hall effect,[1] the intricate connection between edge states[2] and bulk topological index[3] has motivated many novel studies. Hatsugai[4] explicitly showed that the bulk Chern number is identical to the number of edge states for a system with a boundary, which became known as the bulk-edge correspondence. The correspondence also manifests in fractional quantum Hall systems, whose bulk topological order can be detected by the structure of the edge states.[5] The subject enjoyed wider attention after the discovery of quantum spin Hall effect,[6–8] which led to a flourishing field of topological insulators.[9,10] The correspondence between bulk topology and edge states facilitates the classification of topological insulators[11,12] by mapping their boundaries to non-interacting systems subject to Anderson localization.[13,14]

The growing interest of quantum entanglement in condensed matter systems[15] has provided another angle to explore the bulk-edge correspondence. In a non-Abelian fractional quantum Hall system, Li and Haldane[16] emphasized the advantages of revealing bulk topological properties by the whole entanglement spectrum, not just the entanglement entropy alone. They showed that the structure of the entanglement spectrum was identical to that of the edge spectrum of the quantum Hall system. Nontrivial entanglement spectrum can also be generated by real-space partition even in non-interacting integer quantum Hall systems or Chern insulators.[17–21] The intricate connection between entanglement spectra and edge spectra also applies in other topological systems more generally.[15,22–24]

The non-equilibrium quench dynamics of isolated topological systems is another arena for exploring the correspondence between bulk and edge and between edge spectrum and entanglement spectrum. One interesting aspect is the fate of topological edge modes after a quantum quench.[25] Consider a sudden quench of a system from a topologically nontrivial phase to a trivial one. Due to the topological nature of the system, edge states are localized at the boundaries and are expected to be robust for a finite time before they evolve toward the opposite edges and interfere with each other. In the entanglement spectral study of the one-dimensional (1D) Su–Schrieffer–Heeger model, for example, Chung *et al.*[26] found that the two degenerate levels in the middle of the entanglement spectrum is a hallmark of a topological state, which corresponds to a pair of maximally entangled states localized at the edge. The levels remain degenerate for a finite interval, which roughly corresponds to the minimum time it takes at least a bulk quasiparticle-quasihole pair to propagate to the opposite edges. This is also observed in the quench dynamics of a Kitaev chain, in which quasiparticles are Majoranas due to the presence of particle-hole symmetry.[27]

A milestone in quantum simulation is the realization[28] of Haldane's two-dimensional (2D) honeycomb lattice model,[29] which exhibits nontrivial topological aspects in quench dynamics.[30–34] Under unitary evolution, even though the bulk topological number is preserved, the Hall response is not quantized and the edge currents relax to new equilibrium values.[30] Motivated by the intricate connections among topology, dynamics, and quantum entanglement, we study the quench dynamics of the Haldane model using entanglement spectrum, as well as the probability density of selected entanglement eigenstates. We find that there exists a maximum veloc-

*Supported by the National Natural Science Foundation of China (Grant No. 11674282) and the Strategic Priority Research Program of Chinese Academy of Sciences (Grant No. XDB28000000).
**Corresponding author. Email: qlzhang@nit.net.cn
© 2020 Chinese Physical Society and IOP Publishing Ltd

ity that prevents the sudden destruction of the bulk topology. Nevertheless, the 2D dispersion hosts a collection of drastically different velocities that depend on the transverse momentum. They lead to a highly asymmetric evolution of the entanglement spectrum, as well as a sharp contrast in the spatial localization of the different edge modes.

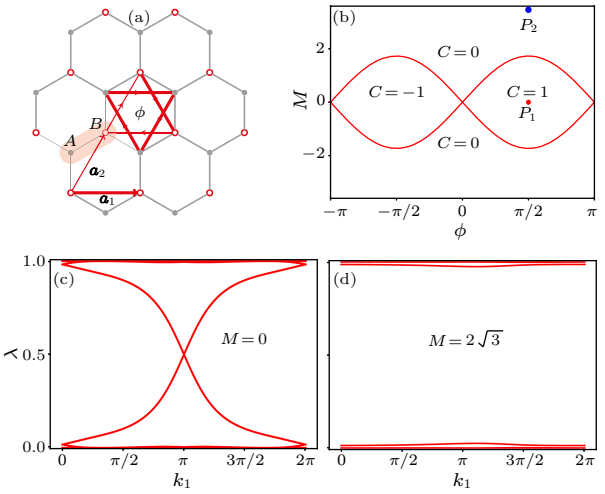

Fig. 1. (a) Two-dimensional honeycomb lattice structure of the Haldane model and our choice of the primitive vectors. (b) The phase diagram of the model with three phases with distinct Chern number. The one-particle entanglement spectrum (OPES) of the half-filled system with (c) $M = 0$ and $\phi = \pi/2$ (topological, pre-quench) and (d) $M = 2\sqrt{3}$ and $\phi = \pi/2$ (non-topological, post-quench). The two sets of parameters are marked as P_1 and P_2 in (b).

Model and Method. We consider Haldane's honeycomb model for the anomalous quantum Hall effect. As illustrated in Fig. 1(a), each unit cell in the Haldane model contains two sites (labelled as A and B) and the primitive vectors can be chosen to be $\boldsymbol{a}_1$ along the horizontal direction and $\boldsymbol{a}_2$ toward another next nearest neighbor. Hopping exists among nearest neighbors with strength t_0, which we set to unity, and among next nearest neighbors, whose strength is fixed to be $t = 1/3$ for simplicity in this study. Due to the nontrivial flux pattern in the model, the next nearest neighbor hopping also contains a phase ϕ or $-\phi$, depending on whether the hopping is along or opposite the arrows in Fig. 1(a). We also introduce inversion symmetry-breaking on-site potential M and $-M$ on A and B sites, respectively. In the momentum space, the model Hamiltonian can be written compactly as

$$H(k_1, k_2) = W(k_1, k_2) + \boldsymbol{B}(k_1, k_2) \cdot \boldsymbol{\sigma}, \qquad (1)$$

in terms of the momentum components k_1 and k_2 along $\boldsymbol{a}_1$ and $\boldsymbol{a}_2$ directions. Here $\boldsymbol{\sigma} = (\sigma_x, \sigma_y, \sigma_z)$ is the vector of Pauli matrices. Explicitly, we have $B_x = -1 - \cos k_1 - \cos k_2$, $B_y = \sin k_1 + \sin k_2$, $B_z = M + (2/3)\sin\phi[\sin k_1 - \sin k_2 + \sin(k_2 - k_1)]$, and $W = -(2/3)\cos\phi[\cos k_1 + \cos k_2 + \cos(k_2 - k_1)]$. We can solve the energy of the two-band model to be $E_\pm(k_1, k_2) = W(k_1, k_2) \pm |\boldsymbol{B}(k_1, k_2)|$. The model at half filling supports a pair of topologically nontrivial phases with Chern number $C = \pm 1$, as shown in Fig. 1(b), in addition to a trivial phase with $C = 0$.

We consider the model with fermions at half filling on a torus geometry under periodic boundary conditions. To reveal the topological properties of the model, we partition the system into two horizontal strips along the zigzag direction and study the entanglement properties of a strip-shaped subsystem with N_2 unit cells across the strip. In the non-interacting system, we calculate the reduced density matrix (RDM) via one-particle correlation functions $C_{mn} = \langle c_m^+ c_n \rangle$ defined on the subsystem.[35–37] The set of eigenvalues λ_i of the correlation matrix is known as the one-particle entanglement spectrum (OPES), which is related to the conventional ES, or the set of eigenvalues ϵ_i of the RDM, as $\lambda_i = 1/(e^{\epsilon_i}+1)$. In other words, the OPES represents the occupation number of the entanglement spectrum at the corresponding filling of the subsystem at a fictitious temperature $T = 1$. For illustration, we compare the OPES for a topological state with $C = 1$ in Fig. 1(c) and that of a trivial state in Fig. 1(d). Note that we exploit the translational symmetry along the strip (the $\boldsymbol{a}_1$ direction), so the spectrum can be characterized by the corresponding momentum k_1. The defining feature of the topological state is a crossing in the spectrum at $\lambda = 1/2$, which arises from the edge modes counter-propagating along opposite edges. However, the location of the crossing at $k_1 = \pi$ is not a topological property and can change as M and ϕ vary.

At half filling the many-body ground state is a Fermi sea of the lower band, $|\text{gs}\rangle = \prod_{l.b.} c^+_{k_1,k_2}|0\rangle$. After the sudden quench to the new H' at $t = 0$, the state evolves as $|\Psi(t)\rangle = e^{-iH't}|\text{gs}\rangle$ and the time-dependent correlation matrix elements evolve as

$$C_{mn}(t) = \langle \text{gs}| e^{iH't} c_m^+ c_n e^{-iH't} |\text{gs}\rangle . \qquad (2)$$

We can then calculate the OPES, or the eigenvalues of the correlation matrix defined on the subsystem, at various t.

Results. In this study we focus on the quench from the topological phase [e.g., $M = 0$ and $\phi = \pi/2$ as marked by P_1 in Fig. 1(b)] to the trivial phase [e.g., $M = 2\sqrt{3}$ and $\phi = \pi/2$ as marked by P_2 in Fig. 1(b)], whose OPESs are shown in Figs. 1(c) and 1(d), respectively. Under a sudden quench from a topological phase to a non-topological phase, the initial state has a high energy compared to the ground state of the post-quench Hamiltonian. Crudely speaking, pairs of entangled quasiparticles and quasiholes are excited from the bulk and propagate toward opposite edges.[38] One can imagine that the system only realizes the topological change when quantum information can be transmitted from one edge to another, in a way like quantum teleportation. In other words, a quasiparticle and quasihole pair generated at the center equidistant from the edges arrive simultaneously at the boundaries at t_c, at which a fictitious measurement at one edge can result in instantaneous message passing to the other, potentially destroying the topological properties of the

dynamical system.

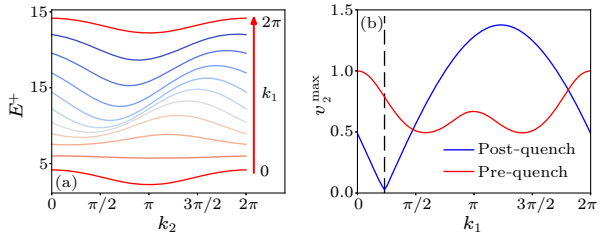

Fig. 2. (a) Energy dispersion of the upper band of the post-quench Hamiltonian along the $\boldsymbol{a}_2$ direction for $k_1 = n\pi/5$ with $n = 0, 1, \ldots, 10$ (from bottom to top). For clarity, the curves are shifted along the energy axis. (b) The maximum group velocity $v_2^{\max}(k_1)$ along the $\boldsymbol{a}_2$ direction for both the pre- and post-quench Hamiltonians. The dashed line at $k_1 = 0.23\pi$ indicates the location of the smallest $v_2^{\max}(k_1)$.

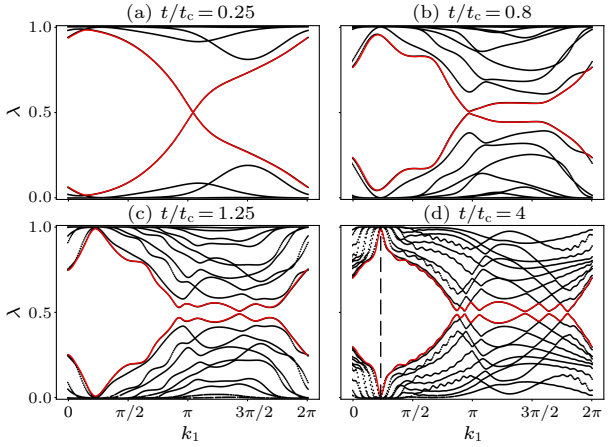

Fig. 3. The OPES of the Haldane model under a sudden quench from the topological phase ($M = 0$) to the trivial phase ($M = 2\sqrt{3}$) with a fixed $\phi = \pi/2$. The spectra are calculated at (a) $t = 0.25t_c$, (b) $t = 0.8t_c$, (c) $t = 1.25t_c$, and (d) $t = 4t_c$ after the quench. The dashed line at $k_1 = 0.23\pi$ in (d) indicates the location of the smallest $v_2^{\max}(k_1)$, as illustrated in Fig. 2(b).

In the 2D case, however, we expect that a family of quasiparticles characterized by momentum k_1 are excited in the bulk upon the topological quench. The velocity along the $\boldsymbol{a}_2$ direction is determined by the 1D dispersion in k_2 (note we set $\hbar = 1$) as $v_2(k_1, k_2) = (\partial/\partial k_2)\, E_+(k_1, k_2)$ for the upper band and similarly for the lower band; they only differ by a sign at our choice of $\phi = \pi/2$. Figure 2(a) shows the k_2 dispersion for 10 different k_1 of the post-quench Hamiltonian. We plot the momentum-dependent maximum post-quench velocity $v_2^{\max}(k_1) \equiv \max_{k_2} |v_2(k_1, k_2)|$ in Fig. 2(b) along with that of the pre-quench Hamiltonian. The characteristic time can then be related to the number of unit cells across the strip N_2 and the maximum post-quench velocity $v_2^{\max} = \max_{k_1} [v_2^{\max}(k_1)]$ as $t_c = N_2/(2v_2^{\max})$, where $v_2^{\max}$ is independent of N_2. This is the minimal time during which the two edges can exchange quasiparticles or quantum information, such that the topological characterization of the state can be changed. In particular, we obtain $t_c \approx 3.62$ for the post-quench Hamiltonian when the subsystem has $N_2 = 10$ unit cells along the $\boldsymbol{a}_2$ direction.

Figure 3 plots the OPES of the 2D system after the quench at time interval (a) $0.25t_c$, (b) $0.8t_c$, (c) $1.25t_c$, and (d) $4t_c$. Here we consider a system with 100 unit cells along $\boldsymbol{a}_2$ and a partition with strip width $N_2 = 10$. At $t = 0.25t_c$ the OPES resembles that of the pre-quench system. In particular, the spectral crossing at $\lambda = 1/2$ remains robust, although its location shifts toward the right. This is a confirmation of the earlier results that the edge states and their spectral crossing, as a signature of the topological phase, are robust right after the sudden quench to a trivial phase. As we mentioned, the momentum of the crossing is not a topological property, and one can see that it shifts slightly to the right.

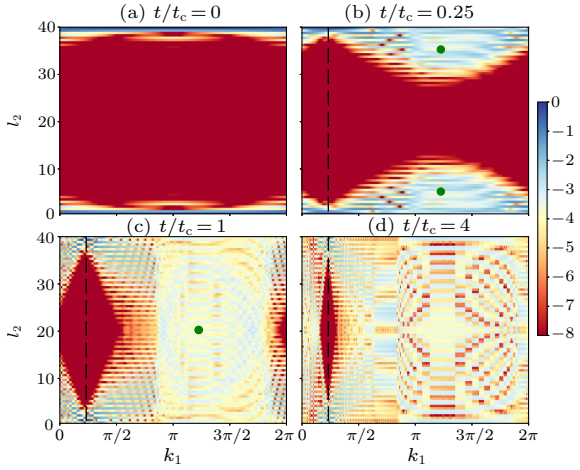

Fig. 4. The logarithm of the total probability density of the two mid-spectral states in the OPES of the Haldane model under a sudden quench from the topological phase ($M = 0$) to the trivial phase ($M = 2\sqrt{3}$) with a fixed $\phi = \pi/2$. The probability density is calculated at (a) $t = 0$, (b) $t = 0.25t_c$, (c) $t = t_c$, and (d) $t = 4t_c$ after the quench. The dashed line at $k_1 = 0.23\pi$ in (b)–(d) indicates the location of the smallest $v_2^{\max}(k_1)$, as illustrated in Fig. 2(b). See main text for the meaning of the green dots.

To help understand the spectral change, we plot the logarithm of the total probability density of the two mid-spectral states $\psi_\pm(k_1, l_2)$ (with $\lambda_\pm$ closest to $1/2$) defined as

$$\ln \rho_{\text{mid}}(k_1, l_2) = \ln \Big[\sum_{i=\pm} |\psi_i(k_1, l_2)|^2 \Big] \qquad (3)$$

in Fig. 4 at time interval (a) 0, (b) $0.25t_c$, (c) t_c, and (d) $4t_c$. Note that in the strip-shaped subsystem we still have translational symmetry along the $\boldsymbol{a}_1$ direction, so k_1 is a good quantum number, while we have open boundary conditions along the $\boldsymbol{a}_2$ direction, along which we use the distance l_2 to describe the wave functions. For smoother plots, we choose a system with 400 unit cells along $\boldsymbol{a}_2$ and a partition with strip width $N_2 = 40$. Figure 4(a) shows that the probability density is distributed mainly near the strip edges, indicating the edge nature of the two states with λ closest to $1/2$ (or entanglement energy closest

to 0). At $t = 0.25t_c$, the probability density remains close to the edges, but a significant spread can be observed around k_1 with the maximum group velocity. Physically, this means that some entangled quasiparticles and quasiholes excited in the bulk have moved across the boundary with the corresponding velocities (as shown in Fig. 2). This causes the increase of entanglement between the two subsystems, which is consistent with the levels of OPES moving toward $\lambda = 1/2$. On the other hand, the quasiparticles distort the edge states, leading to the spread of the probability density of the mid-spectral states. We mark the locations of two classical particles propagating from the edges with the corresponding maximum velocity with the green dots in Fig. 4(b); they locate roughly in the middle of the probability density packets. This is consistent with the light-cone spreading of the edge currents into the interior of the system after quench.[30]

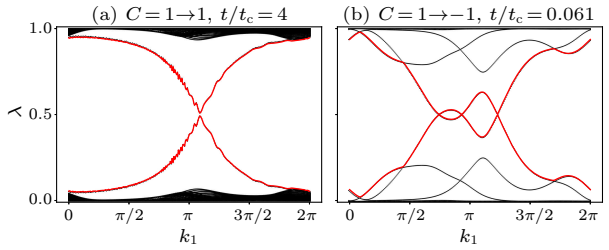

Fig. 5. The OPES of the Haldane model under a sudden quench from $M = 0$ and $\phi = \pi/2$ to (a) $M = 0.5$ and $\phi = \pi/3$ at $t = 4t_c$ and (b) $M = 0.5$ and $\phi = -\pi/3$ at $t = 0.061t_c$. The width of the strip is $N_2 = 40$ unit cells.

Figures 3(b) and 3(c) compare the OPES for $t = 0.8t_c$ and $1.25t_c$. When $t \lesssim t_c$ the crossing near $k_1 \approx \pi$ becomes an anti-crossing. However, the splitting is much smaller than the spacing to other levels, indicating that the concept of topology starts to break down when the finite strip width is felt by the edge-mode propagation. When $t \gtrsim t_c$, edge modes reconstruct and the OPES is featured by oscillations near $\lambda = 1/2$. Figure 4(c) shows $\ln \rho_{\rm mid}(k_1, l_2)$ at $t = t_c$, at which one expects that the fastest quasiparticles and quasiholes excited from the middle arrive at the edges simultaneously. The alternating interference pattern can be observed throughout the strip for the two mid-spectral states with the largest $v_2^{\max}(k_1)$, whose centers are right in the middle of the strip. On the other hand, due to the smallness of the velocity near $k_1 = 0.23\pi$, there is a diamond region with exponentially small probability density. This small-velocity effect persists, as shown in Figs. 3(d) and 4(d) at $t = 4t_c$, though the diamond region devoid of probability density has been further suppressed to a very narrow region. This implies that we can maintain the robustness of certain edge modes by carefully choosing parameters in a quantum quench.

Finally, we mention that if the post-quench Hamiltonian is in the same topological phase, the crossing (or an anti-crossing with a small finite-size gap) in the OPES can be expected to survive in the long-time limit, as shown in Fig. 5(a). On the other hand, if the post-quench Hamiltonian is in a different topological phase (e.g., $C' = -1$), the crossing is still replaced by spectral oscillations at $t \approx t_c$, as for the trivial post-quench Hamiltonian in Fig. 3. Interestingly, we find that the edge modes can reconstruct in a nontrivial way even at $t \ll t_c$, as shown in Fig. 5(b). Though, the total number of crossings at $\lambda = 1/2$ remains to be an odd integer, consistent with its short-time topological nature.

In summary, we have studied the robustness of topological features in the entanglement spectrum of the Haldane model under a sudden quench from a topological state to a trivial state. We find that the quench dynamics of the 2D model is governed by the post-quench momentum dependence of the maximum velocity across the subsystem, which determines the time scale at which the topological characterization of the state is destroyed. Meanwhile, the momentum dependence also leads to a remarkable asymmetry in the OPES and in the probability density of the pair of states that contributes most to the entanglement between the subsystems. This may have potential applications in devices that use the edge modes of a quantum Hall state for information technology.

References

[1] Klitzing K V et al 1980 *Phys. Rev. Lett.* **45** 494
[2] Halperin B I 1982 *Phys. Rev. B* **25** 2185
[3] Thouless D J et al 1982 *Phys. Rev. Lett.* **49** 405
[4] Hatsugai Y 1993 *Phys. Rev. Lett.* **71** 3697
[5] Wen X G 2004 *Quantum Field Theory of Many-Body Systems* (Oxford: Oxford University Press)
[6] Kane C L and Mele E J 2005 *Phys. Rev. Lett.* **95** 226801
[7] Kane C L and Mele E J 2005 *Phys. Rev. Lett.* **95** 146802
[8] Bernevig B A et al 2006 *Science* **314** 1757
[9] Hasan M Z and Kane C L 2010 *Rev. Mod. Phys.* **82** 3045
[10] Qi X L and Zhang S C 2011 *Rev. Mod. Phys.* **83** 1057
[11] Schnyder A P et al 2008 *Phys. Rev. B* **78** 195125
[12] Kitaev A 2009 *AIP Conf. Proc.* **1134** 22
[13] Anderson P W 1958 *Phys. Rev.* **109** 1492
[14] Altland A and Zirnbauer M 1997 *Phys. Rev. B* **55** 1142
[15] See, e.g. Laflorencie N 2016 *Phys. Rep.* **646** 1
[16] Li H and Haldane F D M 2008 *Phys. Rev. Lett.* **101** 010504
[17] Rodríguez I D and Sierra G 2009 *Phys. Rev. B* **80** 153303
[18] Dubail J et al 2012 *Phys. Rev. B* **85** 115321
[19] Huang Z and Arovas D P 2012 arXiv:1205.6266 [cond-mat.str-el]
[20] Huang Z and Arovas D P 2012 *Phys. Rev. B* **86** 245109
[21] Hermanns M et al 2014 *J. Stat. Mech.: Theory Exp.* **2014** P10030
[22] Qi X L et al 2012 *Phys. Rev. Lett.* **108** 196402
[23] Swingle B and Senthil T 2012 *Phys. Rev. B* **86** 045117
[24] Hermanns M 2017 arXiv:1702.01525 [cond-mat.str-el]
[25] See, e.g. Sacramento P D 2017 arXiv:1701.03567 [cond-mat.supr-con]
[26] Chung M C et al 2013 *J. Phys.: Condens. Matter* **25** 285601
[27] Chung M C et al 2016 *Sci. Rep.* **6** 29172
[28] Jotzu G et al 2014 *Nature* **515** 237
[29] Haldane F D M 1988 *Phys. Rev. Lett.* **61** 2015
[30] Caio M D et al 2015 *Phys. Rev. Lett.* **115** 236403
[31] Caio M D et al 2016 *Phys. Rev. B* **94** 155104
[32] Bhattacharya U, Hutchinson J and Dutta A 2017 *Phys. Rev. B* **95** 144304
[33] Mardanya S et al 2018 *Phys. Rev. B* **97** 115443
[34] McGinley M and Cooper N R 2019 *Phys. Rev. B* **99** 075148
[35] Chung M C and Peschel I 2001 *Phys. Rev. B* **64** 064412
[36] Peschel I 2003 *J. Phys. A* **36** L205
[37] Cheong S A and Henley C L 2004 *Phys. Rev. B* **69** 075111
[38] Calabrese P and Cardy J 2016 *J. Stat. Mech.: Theory Exp.* **2016** 064003